Multibranch Bogoliubov-Bloch spectrum of a cigar-shaped Bose condensate in an optical lattice

Tarun Kanti Ghosh
Okayama University

K. Machida
Okayama University

Multibranch Bogoliubov-Bloch spectrum of a cigar-shaped Bose condensate in an optical lattice

Tarun Kanti Ghosh and K. Machida
Department of Physics, Okayama University, Okayama 700-8530, Japan
(Received 31 August 2005; published 18 November 2005)

We study properties of excited states of an array of weakly coupled quasi-two-dimensional Bose condensates by using the hydrodynamic theory. The spectrum of the axial excited states strongly depends on the coupling among the various discrete radial modes in a given symmetry. By including mode coupling within a given symmetry, the complete excitation spectrum of axial quasiparticles with various discrete radial nodes are presented. A single parameter which determines the strength of the mode coupling is identified. The excitation spectrum in the zero angular momentum sector can be observed by using the Bragg scattering experiments.

DOI: 10.1103/PhysRevA.72.053623 PACS number(s): 03.75.Lm, 03.75.Kk, 32.80.Lg

I. INTRODUCTION

The experimental realization of optical lattices [1] is stimulating new perspectives in the study of cold bosons. Optical lattices have enabled us to observe quantum phenomena such as number squeezing [2], collapses and revivals [3], and the diffraction of matter waves [4]. Apart from these examples, BEC in optical lattices are particularly promising physical systems to study the superfluid properties of Bose gases [5,6]. The Bose-Hubbard model has been realized and the quantum phase transition from superfluid to a Mott insulator state was indeed observed experimentally [7–9]. It was predicted that for deep optical lattices the condensate superflow can be lost not only by energetic instability but also by dynamical instability [10–12]. The dynamic instability was verified by the experiments [13]. In a seminal work by Kramer *et al.* [14], they have found the mass renormalization in presence of the optical potential which decreases the value of the axial excitation frequencies. These discrete axial excitation frequencies are experimentally verified [15]. There are several theoretical calculations [16–19] for the sound velocity in a quasi-one-dimensional (1D) Bose gas placed in an 1D optical lattice.

The axial excitations of a cigar shaped condensate can be divided into two regimes: (i) short wavelength excitations where wavelength is much smaller than the axial size and (ii) long wavelength excitations where wavelength is equal or larger than the axial size of the system. In the former case, these excitations can be classified with a continuous wave vector k. However, the finite transverse size of the condensate also produces a discreteness of the spectrum. The short wavelength axial phonons with different number of discrete radial modes of a cigar shaped condensates (without optical lattice) give rise to the multibranch Bogoliubov spectrum (MBS) [20,21]. The MBS was observed in a Bragg spectroscopy with a long duration of the Bragg pulses [22]. An array of weakly coupled quasi-two-dimensional condensates can be created by applying a relatively strong one-dimensional optical lattices to an ordinary three-dimensional cigar shaped condensate along the symmetry axis. In the presence of the periodic lattices, the MBS can be called as multibranch Bogoliubov-Bloch spectrum (MBBS). It is useful to study the MBBS in view of the possibility of the experimental verification. It should be noted that all the modes in a given angular momentum sector are coupled among themselves for any finite value of the axial momentum. For example, when we excite the system to study the sound propagation along the symmetry axis, this perturbation inherently excites all other low energy transverse modes having zero angular momentum. Therefore, all modes are coupled with each other in the same angular momentum sector. Martikainen and Stoof [23] have studied the MBBS only for monopole and lowest energy quadrupole modes without considering the coupling among the various modes within a given symmetry by means of time-dependent Gaussian variational ansatz. Later, Martikainen and Stoof [24] have calculated the spectrum of the phonon and the monopole modes by considering only the coupling between the phonon and the breathing modes. But it is noted that the sound mode is coupled not only with the breathing mode but also with other low-energy modes having zero angular momentum. Similarly, the lowest-energy quadrupole mode is also coupled with other low-energy quadrupole modes. There is a lack of complete study on the MBBS in this system. For complete and correct description of MBBS we have to consider the couplings among all low-energy modes in the same angular momentum sector. In our discretize hydrodynamic description, the couplings among all the modes in the same angular momentum sector are included naturally and we will see in the next section.

In this work we study the excitations in a stack of weakly coupled quasi-two-dimensional condensates. The multibranch Bogoliubov-Bloch spectrum of such system is presented by using the hydrodynamic theory. The MBBS strongly depends on the coupling between the inhomogeneous density in the radial plane and the density modulation along the symmetry axis. Note that one can study only the spectrum of sound, monopole and quadrupole modes without considering the mode coupling completely by using the time-dependent Gaussian variational method. Our discretize hydrodynamic method presented in this paper goes beyond the time-dependent variational method. In principle, we can calculate all low-energy spectrum by including the mode coupling in a given angular momentum sector as long as the excitation energies are less than the chemical potential. We find that the multibranch Bogoliubov-Bloch spectrum changes due to presence of the mode-coupling within a given angular momentum symmetry. Therefore, the mode-coupling should be taken into account while calculating the spectrum correctly.

This paper is organized as follows. In Sec. II, we consider an array of weakly coupled quasi-two-dimensional Bose condensates. Using the discretize hydrodynamic theory, we calculate the multibranch Bogoliubov-Bloch spectrum by including the mode coupling within a given symmetry. We give a brief summary and conclusions in Sec. III.

II. MBBS OF A NON-ROTATING ARRAY OF BOSE CONDENSATES

We assume that the bosonic atoms, at $T=0$, are trapped by an external potential given by the sum of a harmonic trap and a stationary optical potential modulated along the z axis. The Gross-Pitaevskii energy functional can be written as

$$E_0 = \int dV \psi^\dagger(r,z)\left[-\frac{\hbar^2}{2M}\nabla^2 + V_{\rm ho}(r,z) + \frac{g}{2}|\psi(r,z)|^2 + V_{\rm op}(z)\right]\psi(r,z). \quad (1)$$

Here, $V_{\rm ho}(r,z)=(M/2)(\omega_r^2 r^2+\omega_z^2 z^2)$ is the harmonic trap potential and $V_{\rm op}(z)=sE_r\sin^2(qz)$ is the optical potential where $E_r=\hbar^2q^2/2M$ is the recoil energy, s is the dimensionless parameter determining the laser intensity and q is the wave vector of the laser beam. Also, $g=4\pi a\hbar^2/M$ is the strength of the two-body interaction energy, where a is the two-body scattering length. We also assumed that $\omega_r \gg \omega_z$ so that it makes a long cigar shaped trap. The minima of the optical potential are located at the points $z_j=j\pi/q=jd$, where $d=\pi/q$ is the lattice size along the z axis. Around these minima, $V_{op}(z)\sim(M/2)\omega_s^2(z-z_j)^2$, where the layer trap frequency is $\omega_s=\sqrt{s}\hbar q^2/M$. In the usual experiments, the well trap frequency is larger than than the axial harmonic frequency, $\omega_s \gg \omega_z$. Therefore, we can also ignore the harmonic potential along the z-axis since the deep optical lattice dominates over the harmonic potential along the z axis.

The strong laser intensity will give rise to an array of several quasi-two-dimensional condensates. Because of the quantum tunneling, the overlap between the wave functions between two consecutive layers can be sufficient to ensure full coherence. If the tunneling is too small, the strong phase fluctuations will destroy the coherence and lead to a new quantum state, namely Mott insulator state.

In the presence of coherence among the layers it is natural to take the ansatz for the wave function as

$$\psi(x,y,z) = \sum_j \psi_j(x,y) f(z-z_j). \quad (2)$$

Here, $\psi_j(x,y)$ is the wave function of the two-dimensional condensate at the site j and $f(z-z_j)$ is a localized function at jth site. The localized function can be written as

$$f(z-z_j) = \left(\frac{M\omega_s}{\pi\hbar}\right)^{1/4} e^{-(M\omega_s/2\hbar)(z-z_j)^2}. \quad (3)$$

Substituting the above ansatz into the energy functional and considering only the nearest-neighbor interactions, one can get the following energy functional:

$$E_0 = \sum_j \int dxdy\left[-\frac{\hbar^2}{2M}\psi_j^\dagger \nabla_r^2 \psi_j + V_{\rm ho}|\psi_j|^2\right] + \frac{g_{2D}}{2}\sum_j \int dxdy\,\psi_j^\dagger\psi_j^\dagger\psi_j\psi_j - J\sum_{j,\delta=\pm1}\int dxdy[\psi_{j+\delta}^\dagger\psi_j + \psi_j^\dagger\psi_{j+\delta}]. \quad (4)$$

Here, J is the strength of the Josephson coupling between adjacent layers which is given as

$$J = -\int dz f(z)\left[-\frac{\hbar^2}{2M}\nabla_z^2 + V_{\rm op}(z)\right] f(z+d) \sim \hbar\omega_r\left(\frac{\pi a_r}{\sqrt{2}\lambda}\right)^2(\pi^2-4)se^{-\pi^2\sqrt{s}/4}, \quad (5)$$

where $a_r=\sqrt{\hbar/M\omega_r}$. Also, the strength of the effective on-site interaction energy is $g_{2D}=g\int dz|f_0(z)|^4=4\sqrt{\pi/2}(\hbar^2/M)\times(a/a_s)$, where $a_s=\sqrt{\hbar/M\omega_s}$. Equation (4) shows that each layer j is coupled with the nearest-neighbor layers $j\pm1$ through the tunneling energy J. The axial dimension appears through the Josephson coupling between two adjacent layers. The Hamiltonian corresponding to the above energy functional is similar to an effective 1D Bose-Hubbard Hamiltonian in which each lattice site is replaced by a layer with radial confinement.

The Heisenberg equation of motion for the bosonic order parameter is

$$i\hbar\dot{\psi}_j = \left[-\frac{\hbar^2}{2M}\nabla_r^2 + V_{\rm ho} + g_{2D}\psi_j^\dagger\psi_j\right]\psi_j - J(\psi_{j-1}+\psi_{j+1}). \quad (6)$$

Using the phase-density representation of the bosonic field operator as $\psi_j=\sqrt{n_j}e^{i\theta_j}$ and neglecting the quantum pressure term, one can get the following equations of motion for the density and phase:

$$\dot{n}_j = -\frac{\hbar}{M}\nabla_r\cdot(n_j\nabla_r\theta_j) + \frac{2J}{\hbar}[\sqrt{n_jn_{j-1}}\sin(\theta_j-\theta_{j-1}) - \sqrt{n_jn_{j+1}}\sin(\theta_{j+1}-\theta_j)] \quad (7)$$

and

$$\hbar\dot{\theta}_j = -\frac{\hbar^2}{2M}(\nabla_r\theta_j)^2 + J\left[\sqrt{\frac{n_{j+1}}{n_j}}\cos(\theta_{j+1}-\theta_j) + \sqrt{\frac{n_{j-1}}{n_j}}\cos(\theta_j-\theta_{j-1})\right] - V_{\rm ho} - g_{2D}n_j. \quad (8)$$

Here, "˙" represents the time derivative. In equilibrium, the condensate density at each layer is $n_0(r)=[\mu_0-V_{\rm ho}(r)]/g_{2D}$, where we have neglected the effect of the tunneling energy J since it is very small in the deep optical lattice regime. Also, $\mu_0=\hbar\omega_r\sqrt{8/\pi}(Na/a_s)$ is the chemical potential at each layer, where N is the number of atoms at each layer. In this system, we have two energy scales: the chemical potential of each layer $\mu_0\sim s^{1/8}$ which is associated with the radial plane and the tunneling energy $J\sim se^{-\sqrt{s}}$ which is associated with the density modulation along the z axis. The strength of the

chemical potential can be enhanced by increasing the lattice depth or by increasing the number of atoms. The tunneling energy J decreases with the increasing of the lattice depth.

We linearize the hydrodynamic equations around the equilibrium state, as $n_j = n_0 + \delta n_j$ and $\theta_j = \delta\theta_j$. The equations of motion for the density and phase fluctuation becomes

$$\delta\dot{n}_j = -\frac{\hbar}{M}\nabla_r \cdot [n_0(r)\nabla_r \delta\theta_j] + \frac{2J}{\hbar} n_0(r)[2\delta\theta_j - \delta\theta_{j-1} - \delta\theta_{j+1}] \tag{9}$$

and

$$\hbar\,\delta\dot{\theta}_j = -g_{2D}\delta n_j - \frac{J}{2n_0(r)}[2\delta n_j - \delta n_{j-1} - \delta n_{j+1}]. \tag{10}$$

Note that the second term of the right hand side of Eq. (10) is proportional to the small parameter J and inversely proportional to the large parameter $n_0(r=0) = \mu_0/g_{2D}$. Therefore, we can neglect the term which is proportional to the $J/2n_0(r)$. After some algebra, we get second order equation of motion for the density fluctuation as

$$\delta\ddot{n}_j = \frac{g_{2D}}{M}\nabla_r \cdot [n_0(r)\nabla_r \delta n_j] - \frac{2Jg_{2D}}{\hbar^2} n_0(r)[2\delta n_j - \delta n_{j-1} - \delta n_{j+1}]. \tag{11}$$

The above equation tells us that the density fluctuation at each layer j is coupled with the nearest-neighbor layers $j \pm 1$. We seek the normal mode solutions of the density fluctuations at layer j in the following form:

$$\delta n_j = \delta n(r) e^{i[jkd - \omega_l(k)t]}. \tag{12}$$

Here, k is Bloch wave vector (quasi-momentum) of the excitations. The Bloch wave vector p which is associated with the velocity of the condensate in the optical lattice is set to zero.

Substituting the above equation into Eq. (11), we get

$$-\omega_l^2(k)\delta n = \frac{g_{2D}}{M}\nabla_r \cdot (n_0 \nabla_r \delta n) - \frac{8Jg_{2D}}{\hbar^2} n_0(r)\sin^2(kd/2)\delta n, \tag{13}$$

where l is a set of two quantum numbers: radial quantum number, n_r and the angular quantum number m. The parameter $J\mu$ in front of the $\sin^2(kd)$ term determines the strength of the coupling between the inhomogeneous density in the radial plane and the density modulation along the z axis.

For $k=0$, the solutions are known exactly and analytically [25]. The energy spectrum and the normalized eigen functions, respectively, are given as, $\omega_l^2 = \omega_r^2[|m| + 2n_r(n_r + |m| + 1)]$ and

$$\delta n(r,\phi) = \frac{(1 + 2n_r + |m|)^{1/2}}{(\pi R_0^2)^{1/2}} \tilde{r}^{|m|} P_{n_r}^{(|m|,0)}(1 - 2\tilde{r}^2) e^{im\phi}. \tag{14}$$

Here, $P_n^{(a,b)}(x)$ is the Jacobi polynomial of order n and ϕ is the polar angle. The radius of each condensate layer is $R_0 = 2\mu_0/M\omega_r^2$ and $\tilde{r} = r/R_0$ is the dimensionless variable.

The solution of Eq. (13) can be obtained for arbitrary value of k by numerical diagonalization. For $k \neq 0$, we can expand the density fluctuations as

$$\delta n(r) = \sum_l b_l \delta n_l(r,\phi). \tag{15}$$

Substituting the above expansion into Eq. (13), we obtain

$$0 = [\tilde{\omega}_l^2 - [|m| + 2n_r(n_r + |m| + 1)] - B_0\sin^2(kd/2)]b_l + B_0\sin^2(kd/2)\sum_{l'} M_{ll'} b_{l'}, \tag{16}$$

where $\tilde{\omega}_l = \omega_l/\omega_r$ and the dimensionless parameter B_0 is defined as

$$B_0 = \frac{8J\mu_0}{\hbar^2\omega_r^2}. \tag{17}$$

The matrix element $M_{ll'}$ is given by

$$M_{ll'} = \frac{(1 + 2n_r + |m|)}{\pi}\int d^2\tilde{r}\tilde{r}^{2+|m|+|m'|} e^{i(m-m')\phi} \times P_{n_r'}^{(|m'|,0)}(1 - 2\tilde{r}^2) P_{n_r}^{(|m|,0)}(1 - 2\tilde{r}^2). \tag{18}$$

The above eigenvalue problem is block diagonal with no overlap between the subspaces of different angular momentum, so that the solutions to Eq. (16) can be obtained separately in each angular momentum subspace. We can obtain all low-energy multibranch Bogoliubov-Bloch spectrum from Eq. (16) which is our main result. Equations (16) and (18) show that the spectrum depends on average over the radial coordinate and the coupling among the modes within a given angular momentum symmetry for any finite value of k. Particularly, the couplings among all other modes are important for large values of kd and B_0. It is interesting to note that the curvature of a mode spectrum depends on a single parameter B_0 which is defined in Eq. (17). The parameter B_0 can remain unchanged by changing values of the J and μ_0 in a various combination. Therefore, the curvatures of the spectrum of a given mode for various combinations of J and μ_0 with fixed B_0 are the same.

Before presenting the exact numerical results, we make some approximation for a quantitative discussions. If we neglect the couplings among all other modes in the $m=0$ sector by setting $l' = (n_r, 0)$ in Eqs. (16) and (18), one can easily get following spectrum:

$$\tilde{\omega}_{n_r}^2 = 2n_r(n_r + 1) + (1 - M_{n_r,n_r})B_0\sin^2(kd/2). \tag{19}$$

The above equation can also be obtained by using first-order perturbation theory to Eq. (13). In the limit of long wavelength, the $n_r=0$ mode is phonon like with a sound velocity $c_0 = \sqrt{\mu_0/2M^*}$, where $M^* = \hbar^2/2Jd^2$ is the effective mass of the atoms in the optical potential. This sound velocity exactly matches with the result obtained in Ref. [14] and is similar to the result obtained without optical potential [20]. This sound velocity is smaller by a factor of $\sqrt{2}$ with respect to the sound velocity obtained previously [16–19] for quasi-1D Bose gas placed in an optical potential. This is due to the effect of the average over the radial variable which can be seen from Eqs.

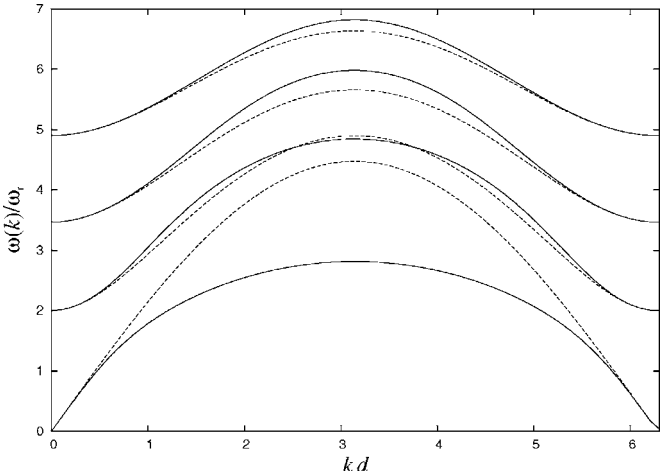

FIG. 1. Plots of the low-energy Bogoliubov-Bloch modes in the $m=0$ sector. Here, $J=0.1\hbar\omega_r$ and $\mu_0=50\hbar\omega_r$. Solid and dashed lines are obtained from Eqs. (16) and (19), respectively

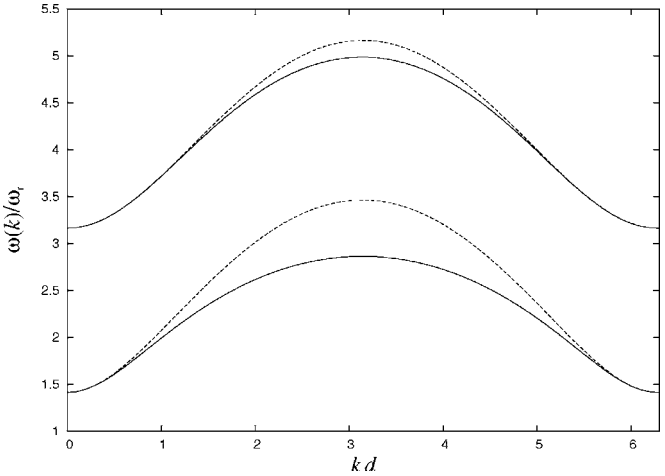

FIG. 2. Plots of the low-energy Bogoliubov-Bloch modes in the $m=\pm 2$ sector. Here, $J=0.1\hbar\omega_r$ and $\mu_0=50\hbar\omega_r$. Solid and dashed lines are obtained from Eqs. (16) and (20)

(16) and (18). In Fig. 1 we show few low-energy multibranch Bogoliubov-Bloch spectrum in the $m=0$ sector as a function of kd by solving the matrix (16).

The lowest branch corresponds to the Bogoliubov-Bloch axial mode with no radial nodes. This mode has the usual form $\omega_r=c_s k$ at low momenta, where c_s is the real sound velocity. Note that $c_s \lesssim c_0$ which implies that the dispersion relations are modified due to the coupling among all other modes. The changes in the spectrum is clearly visible in the central part of the Brillouin zone. This is due to the fact that the mode coupling is strong enough in the central part of the Brillouin zone due to the particular nature of the k-dependent part [see Eq. (16)]. The second branch corresponds to one radial node and starts at $2\omega_r$ for $k=0$. The breathing mode has the free-particle dispersion relation and it can be written in terms of the effective mass (m_b^*) of this mode as $\omega_2(k)=2\omega_r+\hbar k^2/2m_b^*$. Figure 1 shows that the mode coupling does not affect the breathing mode spectrum appreciably. The third and fourth lowest-energy modes are also given in Fig. 1. These modes are also changed in the central part of the Brillouin zone due to the mode coupling. One could see from Fig. 1 that the effective masses of each modes are different. The group velocity along the z direction deviates from its long-wavelength limit when $kd \sim \pi$. The mode coupling induced by the $\sin^2(kd)$ perturbation in Eq. (11) becomes more significant with increasing k and has the effect of lowering the sound speed. This coupling is associated with the interplay of the density modulation along the z direction and the strong inhomogeneity of the equilibrium density in the radial direction in each plane. The effective masses are negative when $kd > \pi$.

The coupling between the transverse quadrupole modes ($m=\pm 2$) and the modes in the $m \neq \pm 2$ sector does not exist since these modes are orthogonal to each other as it can be seen from Eq. (18). However, the lowest energy quadrupole spectrum ($n_r=0, m=\pm 2$) strongly depends on other low-energy quadrupole modes with various discrete radial nodes ($n_r \neq 0, m=\pm 2$). We neglect the couplings among all other modes in the $m=\pm 2$ sector by setting $l'=(n_r,2)$ in Eqs. (16) and (18), then one can easily get following spectrum:

$$\tilde{\omega}_{n_r}^2 = 2 + 2n_r(n_r+3) + (1 - M_{n_r,2;n_r,2})B_0 \sin^2(kd/2). \tag{20}$$

In Fig. 2, we present first two low-energy MBBS for quadrupole modes. Figure 2 clearly shows that the mode-coupling also reduces the spectrum for the quadrupole modes in the central part of the Brillouin zone. In Ref. [23], the spectrum for the breathing and the lowest energy quadrupole modes are obtained analytically within the Gaussian variational analysis. The mode coupling was not considered in this variational analysis [23]. In Fig. 3, we compare the spectrum of the breathing and lowest energy quadrupole modes obtained from Eq. (16) with those of obtained in Ref. [23]. It is clear from Fig. 3 that the mode-coupling reduces the spectrum strongly and it should be taken into account for calculating the spectrum correctly.

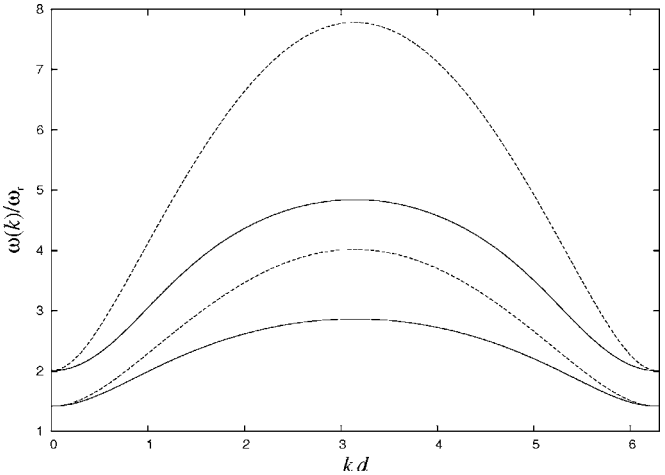

FIG. 3. Plots of the spectrum of breathing and lowest-energy quadrupole modes. Here, $J=0.1\hbar\omega_r$ and $\mu_0=50\hbar\omega_r$. Solid and dashed lines are obtained from Eq. (16) and Ref. [23], respectively

III. SUMMARY AND CONCLUSIONS

In this work, we have studied excitation energies of the axial quasiparticles with various discrete radial nodes of an array of weakly coupled quasi-two-dimensional Bose condensates. Our discretize hydrodynamic description enables us to produce correctly all low-energy MBBS by including the mode couplings among different modes within the same angular momentum sector. We found that the mode coupling strongly changes the spectrum. Therefore, it should be taken into account to calculate such spectrum correctly. The mode coupling is strong enough in the central part of the Brillouin zone. The single parameter B_0, defined in Eq. (17), is identified which is always associated with the k-dependent part and it scales with the product of two energy scales of this system, namely, J and μ_0. The parameter B_0 is a good measure for determination of the effect of the optical lattices on the spectrum. Particularly, the spectrum for the phonon and breathing modes can be observed in a Bragg scattering experiments [26] as discussed below. The MBBS can be observed in the Bragg scattering experiments as the MBS was observed in Ref. [22]. Due to the axial symmetry, the modes having only zero angular momentum can be excited in the Bragg scattering experiments. In the Bragg spectroscopy, the condensate is excited by an external moving optical potential $V=V_B(t)\cos(kz-\omega t)$, where $V_B(t)$ is the intensity of the Bragg pulses. This optical potential is created by using two Bragg pulses with approximately parallel polarization, separated by an angle θ. The pulses have a frequency difference ω determined by two acousto-optic modulators. The wave vector $\mathbf{k}$ is adjusted to be along the z axis. Both the values of k and ω can be tuned by changing the angle between two beams and varying their frequency difference. For small values of k the system is excited in the phonon regime and the response is detected by measuring the net momentum $P_z(\omega,k)$ imparted to the system by the Bragg pulses. The multibranch Bogoliubov spectrum is obtained by observing the locations of the peaks in $P_z(\omega,k)$ for various values of k. The frequency ω must be comparable to radial trap frequency ω_r in order to excite the breathing and other modes. The duration of the Bragg pulses must be larger than the radial trapping period $T_B>2\pi/\omega_r$ in order to have large populations of the radial quasiparticle states.

ACKNOWLEDGMENTS

This work was supported by a grant (Grant No. P04311) of the Japan Society for the Promotion of Science.

[1] B. P. Anderson and M. A. Kasevich, Science **282**, 1686 (1998).
[2] C. Orzel, A. K. Tuchman, M. L. Fenselau, M. Yasuda, and M. A. Kasevich, Science **291**, 2386 (2001).
[3] M. Greiner, O. Mandel, T. W. Hansch, and I. Bloch, Nature (London) **419**, 51 (2002).
[4] Y. B. Ovchinnikov, J. H. Muller, M. R. Dorey, E. J. D. Vredenbregt, K. Helmerson, S. L. Rolston, and W. D. Philips, Phys. Rev. Lett. **83**, 284 (1999).
[5] F. S. Cataliotti, S. Burger, C. Fort, P. Maddaloni, F. Minardi, A. Trombettoni, A. Smerzi, and M. Inguscio, Science **293**, 843 (2001).
[6] S. Burger, F. S. Cataliotti, C. Fort, F. Minardi, M. Inguscio, M. L. Chiofalo, and M. P. Tosi, Phys. Rev. Lett. **86**, 4447 (2001).
[7] D. Jaksch, C. Bruder, J. I. Cirac, C. W. Gardiner, and P. Zoller, Phys. Rev. Lett. **81**, 3108 (1998).
[8] D. van Oosten, P. van der Straten, and H. T. C. Stoof, Phys. Rev. A **63**, 053601 (2001).
[9] M. Greiner, O. Mandel, T. Esslinger, T. W. Hansch, and I. Bloch, Nature (London) **415**, 39 (2002).
[10] B. Wu and Q. Niu, Phys. Rev. A **64**, 061603(R) (2001).
[11] V. V. Konotop and M. Salerno, Phys. Rev. A **65**, 021602(R) (2002).
[12] A. Smerzi, A. Trombettoni, P. G. Kevrekidis, and A. R. Bishop, Phys. Rev. Lett. **89**, 170402 (2002).
[13] F. S. Catalioti, L. Fallani, F. Ferlaino, C. Fort, P. Maddaloni, and M. Inguscio, New J. Phys. **5**, 71 (2003); L. Fallani, L. De Sarlo, J. E. Lye, M. Modugno, R. Saers, C. Fort, and M. Inguscio, Phys. Rev. Lett. **93**, 140406 (2004).
[14] M. Kramer, L. Pitaevskii, and S. Stringari, Phys. Rev. Lett. **88**, 180404 (1998).
[15] C. Fort, F. S. Cataliotti, L. Fallani, F. Ferlaino, P. Maddaloni, and M. Inguscio, Phys. Rev. Lett. **90**, 140405 (1998).
[16] K. Berg-Sorensen and K. Molmer, Phys. Rev. A **58**, 1480 (1998).
[17] J. Javanainen, Phys. Rev. A **60**, 4902 (1999).
[18] M. Machholm, C. J. Pethick, and H. Smith, Phys. Rev. A **67**, 053613 (2003).
[19] E. Taylor and E. Zaremba, Phys. Rev. A **68**, 053611 (2003).
[20] E. Zaremba, Phys. Rev. A **57**, 518 (1998).
[21] P. O. Fedichev and G. V. Shlyapnikov, Phys. Rev. A **63**, 045601 (2001).
[22] J. Steinhauer, N. Katz, R. Ozeri, N. Davidson, C. Tozzo, and F. Dalfovo, Phys. Rev. Lett. **90**, 060404 (2003).
[23] J. P. Martikainen and H. T. C. Stoof, Phys. Rev. A **68**, 013610 (2003).
[24] J. P. Martikainen and H. T. C. Stoof, Phys. Rev. A **69**, 023608 (2004).
[25] M. Fliesser, Andras Csordas, P. Szepfalusy, and R. Graham, Phys. Rev. A **56**, R2533 (1997); P. Ohberg, E. L. Surkov, I. Tittonen, S. Stenholm, M. Wilkens, and G. V. Shlyapnikov, *ibid.* **56**, R3346 (1997).
[26] J. Stenger, S. Inouye, A. P. Chikkatur, D. M. Stamper-Kurn, D. E. Pritchard, and W. Ketterle, Phys. Rev. Lett. **82**, 4569 (1999); D. M. Stamper-Kurn, A. P. Chikkatur, A. Gorlitz, S. Inouye, S. Gupta, D. E. Pritchard, and W. Ketterle, *ibid.* **83**, 2876 (1999).